Available online at www.eccomasproceedia.org
Eccomas Proceedia COMPDYN (2017) 101-119

ECCOMAS
Proceedia

COMPDYN 2017
6th ECCOMAS Thematic Conference on
Computational Methods in Structural Dynamics and Earthquake Engineering
M. Papadrakakis, M. Fragiadakis (eds.)
Rhodes Island, Greece, 15–17 June 2017

CYCLIC EARTHQUAKE-TYPE PERFORMANCE OF ONE-BAY SINGLE-STORY REINFORCED CONCRETE (R/C) FRAMES RETROFITTED WITH AN ENCASED R/C PANEL

G. C. Manos[1], V. Soulis[2], K. Katakalos[2], G. Koidis[3], M. Theofanous[4]

[1] Professor and ex-Director of the Lab. of Strength of Materials and Structures, Aristotle University
e-mail: gcmanos@civil.auth.gr

[2] Dr. Civil Engineer, Research Ass., Lab. of Strength of Materials and Structures, Aristotle University
e-mail: vassilios_soulis@yahoo.com; katakaloskostas@gmail.com

[3] Postgraduate student, Lab. of Strength of Materials and Structures, Aristotle University
e-mail: george_florina@hotmail.com

[4] Lecturer in Structural Engineering, Dept. Civil Engineering, University of Birmingham
e-mail: m.theofanous@bham.ac.uk

Keywords: Retrofitting, Reinforced Concrete Frames, Encasement R/C Panels, Jacketing, Soft Ground Floor

Abstract. *The in-plane behaviour of one-bay single-story reinforced concrete (R/C) frames, retrofitted by jacketing of their columns together with a cast-in-place encased R/C panel, was studied numerically when subjected to cyclic seismic-type horizontal loading. The influence of such an encased R/C panel is examined, when it is connected with the surrounding frame with or without steel ties. From preliminary numerical results is concluded that an encased panel results in a considerable increase of the stiffness and the bearing capacity of such a system, especially when steel ties are present at the interface. The presence of steel ties moderates the amplitude of the forces transferred at the narrow column-to-beam joint regions in a direction normal to the interface through the contact/gap mechanism; thus it, mitigates the possibility of crushing the encased panel and/or parts of the columns or beams at these regions. Thus, an encased R/C panel connected by the appropriate steel ties with the surrounding R/C frame, has a beneficial effect on the seismic behaviour of this type of structural system. Experiments were performed in order to quantify the behaviour of such steel tie connections at the interface under a stress field similar to the one that develops at this part of the encasement during seismic type loading. Such measured behaviour is in agreement with the assumptions made concerning the behavioural characteristics of these steel ties in the preliminary numerical analysis. Next, simple and advanced numerical simulations of the tested connection detail are also examined in an effort to validate numerical tools that can serve the purpose to quantify such a transfer of forces for connection details that can be used in design. It was concluded that the described advanced numerical simulation is a quite valid numerical approach.*

Peer-review under responsibility of the organizing committee of COMPDYN 2017.
doi: 10.7712/120117.5411.16890

1 INTRODUCTION

Many multi-story reinforced concrete (R/C) structures, built in seismic regions, have their ground floor designed to function as a parking space. Therefore, the bays of the R/C frames at this level are left without masonry infills whereas all the stories above have their corresponding bays of the R/C frames infilled with external masonry walls or with internal masonry partitions (figures 1a and 1b). It was demonstrated by extensive past research ([1]) that the dynamic and earthquake behaviour of such structures, having a relatively flexible ground floor (soft story) and stiff upper stories, results in increased demands on the structural elements of the ground floor. This is due to the interaction of the masonry infills with the surrounding R/C frames that contributes to a substantial increase of the story stiffness of these upper stories compared to the story stiffness of the ground floor ([1], [2], [3]).

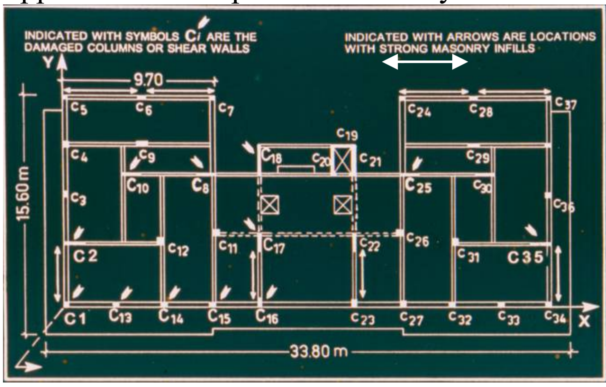

Figure 1a. Plan of the “soft story” of the “Pyrgos Hardas” building [1].

Figure 1b. Temporary shoring of the damaged “soft story” of the “Pyrgos Hardas” building [1].

Figure 1c. Heavily damaged columns at the soft story Athens 1999 [1].

Figure 1d. Temporary shoring by encasing the columns and filling the bay with steel diagonals [1].

This, in turn, leads to structural damage (figure 1c), unless the structural R/C elements at the ground floor are properly designed [1, 2, 3, 4, 5]. As this behaviour was not well understood in the past, there are many structures with such a soft storey that were designed and constructed with their R/C structural elements now in need of upgrading their capacity. Figures 1b and 1d depict temporary shoring schemes using either wooden or steel structural elements. These temporary shoring schemes serve primarily to secure the transfer of the gravitational forces at the “soft story” level despite the damaged columns or shear walls thus safeguarding against partial or total collapse. At the same time with the encasement of the damaged columns themselves (figure 1d) as well as with filling the bay within two columns with wooden or steel diagonals (figures 1b or 1d, respectively), aim to increase the stiffness at the resisting capacity of the soft story to the shear forces generated by the seismic action. Such temporary shoring schemes should be deployed as soon as possible as their contribution can be critical in ensuring the structural stability of such damaged building in the aftermath of a strong earthquake main shock that is usually followed by a series of quite strong aftershocks. This contribution of the depicted in figures 1b and 1d temporary shoring schemes can be enhanced even further by retrofitting schemes, which will replace the temporary shoring and will increase the stiffness and the resistance of the "soft story" becoming a permanent part of the structural system. Such a retrofitting scheme is studied here. It can be easily applied to such a soft ground floor of multi-storey R/C structures [4, 5, 6, 7, and 8]. Initially, a retrofitting effort usually consists of repairing and strengthening the structural elements at the soft ground floor by:

- R/C jacketing of the existing R/C columns at the ground floor level (figure 2a).

- R/C jacketing of the existing R/C beams at the ground floor level.

With the jacketing of these ground floor structural elements, a certain increase in their strength and ductility is expected to be achieved. The current Greek guidelines for retrofitting reinforced concrete buildings [8], also provides for the addition of an R/C panel that can be added as an encasement, filling the space between the jacketed columns and beams (figure 2b).

Figure 2a. Damaged columns at the soft story being strengthened with R.C. jacketing

Figure 2b. Damaged columns at the soft ground floor being encased with a R/C panel filling up the bay.

In the relevant provisions of these guidelines [8] the designer is provided with a number of distinct choices. In the present investigation the following choices will be studied:

a. The encased R/C panel is not structurally connected to the surrounding R/C structural elements within (columns or beam). Alternatively, a limited connection is described between the R/C panel and the upper/lower horizontal frame interface.

b. The encased R/C panel is constructed together with a connection with the surrounding R/C structural elements strengthened by jacketing within a bay (columns or beam), utilizing steel ties. In this case, the thickness of the encased R/C panel is smaller than the width of the beams that form the encased bay.

2 PRELIMINARY NUMERICAL SIMULATION

The numerical study that is presented in this section was limited to examining a single-storey one-bay R/C frame (figure 3) formed by two columns (left and right) and two beams (top and bottom). The over-all frame dimensions, chosen arbitrarily, were: The length between the mid axes of the two columns equal to 6m. The height between the mid-axes of the top and bottom beams equal to 3m. The cross section of the columns 340mm x 340mm; that of the top beam 300mm x 600mm and that of the bottom beam with large flexural stiffness representing a rather stiff foundation. The numerical model included three non-linear springs located at all the joints between the columns and the beams either at the top and bottom of each column or at the left and right side of each beam, whereas the region representing the actual beam-column joint was assumed non-deformable. These non-linear springs were provided with tri-linear moment-rotation proper-ties thus representing the possibility of plastic hinges forming there. The properties of these moment-rotation springs were derived considering typical rein-forcing details for the columns and beams for such structural elements at the ground floor; an axial force level for each column equal to 510 KN, representing the axial force for a building with three more stories above the ground floor where the examined single-storey one bay R/C sub-assembly is assumed to be located. In this way, only the flexural non-linear behaviour scenario, by the formation of the plastic hinges is considered, excluding any shear non-linear behaviour of the R/C structural members. In this preliminary numerical simulation, the behav-iour of the encased R/C panel itself was considered to be elastic. A subsequent numerical simulation considered the possibility of non-linear behaviour of the encased R/C panel itself. The properties of these moment-rotation springs were derived considering typical reinforcing details for the columns and beams for such structural elements at the ground floor as well as an axial force level for the columns equal to 510 KN, representing the axial force level for a building with three more stories above the ground floor where the examined single-storey one bay R/C sub-assembly is assumed to be located. The thickness of the encased R/C panel was assumed to be equal to 150mm constructed with a material having Young's modulus equal to E=7GPa to account for a level of pre-cracking.

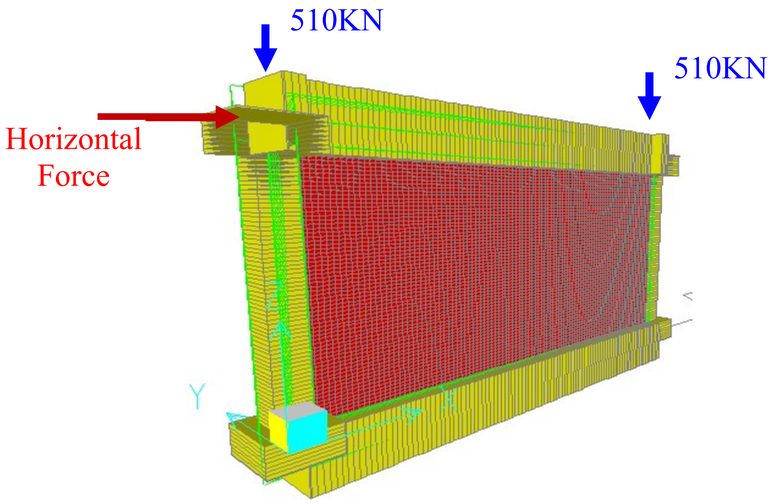

Figure 3. Single-story one bay R/C frame with the encased R/C panel

2.1. Numerical models.

The following three alternative numerical models are examined ([6], [7]).

a) The first numerical model was that without any encasement ("bare model").

b) In the previous "bare model" an encased R/C panel is added having a 150mm thickness. This panel was connected to the surrounding frame with non-linear link elements, which represent the contact/gap mechanism between the encased panel and the surrounding frame. Through this mechanism only forces normal to the interface are transferred between the encased panel and the surrounding frame ([6], [7]). This is denoted as "encased model b".

c) Again to the "bare model" an encased R/C panel is added having a 150mm thickness. However, this time the panel was connected to the surrounding frame with two distinct types of non-linear link elements each one representing a distinct force transfer mechanism ([6], [7]). The first type of link represents again the contact/gap mechanism between the R/C panel and the surrounding frame, as explained before. The second type of connection between the R/C encasement panel and the surrounding frame represents an additional force transfer mechanism that simulates the presence of a steel metal tie. This second type of link was assumed to have an elasto-plastic behaviour in its longitudinal direction, representative of a steel reinforcing bar with a diameter of 12mm and a yield stress of 500MPa. Similar elasto-plastic behaviour was also assumed in the tangential direction representing such tangential behaviour of a 12mm diameter tie. Towards the quantification of such tangential behaviour of a steel tie, a sequence of tests was conducted that will be briefly described in section 4. The results that are presented here correspond to an encased R/C panel that is connected with the surrounding columns and beams with both the contact/gap and the steel metal ties mechanisms. The behaviour of the following three distinct models was studied that included an encasement of an R/C panel within the one-storey one bay R/C frame. This is denoted as "encased model c".

2.2. Numerical results

All numerical models were subjected to a horizontal incremental force in a direction coinciding with the mid-axis of the top beam (figure 3) in a "push - over" type of loading. The following non-linear mechanisms were considered:

-The possibility of developing plastic hinges at the top and bottom of the columns as well as at the left and right edge of the top beam.

-The possibility to triggering the contact/gap mechanism at the interface between the encased panel and the surrounding R/C frame in the direction normal to the interface between the encased panel and the surrounding R/C structural elements (either top/bottom beam or lefty/right column).

-The possibility of the steel ties connecting the encased panel with the top and bottom beam and the left and right column behaving in an elasto-plastic way both in a direction normal as well as tangential to the interface.

These non-linear mechanisms were not extended to include the R/C panel itself at this preliminary numerical analysis. Such a non-linear behaviour was included in a subsequent simulation. The numerical results include: a) the variation of the applied horizontal force against the corresponding displacement, b) the deformed shape of the single-storey one bay frame with or without the encasement at the maximum deformation level at the end of the "push – over" loading sequence, c) the variation of the forces that develop at the interface between the encased panel and the surrounding R/C frame.
Figures 4a and 4b depict the numerically predicted behaviour for the "bare model". The non-linearity in the curve representing the variation of the applied horizontal force at the axis of the top beam against the corresponding displacement, as depicted in figure 4a, is quite evident

when the horizontal displacement exceeds the value of 15mm. When the top beam horizontal displacement level reaches the maximum amplitude of 24.5mm, plastic hinges develop at the critical locations of the beams and columns, as depicted in figure 4b. The maximum amplitude of the horizontal force at that level is 174KN which represents the bearing capacity of the bare frame whereas its initial stiffness is approximately 10KN/mm. The above frame performance is dominated by flexure, a fact that presumes that all structural elements are provided with the appropriate shear resistance.

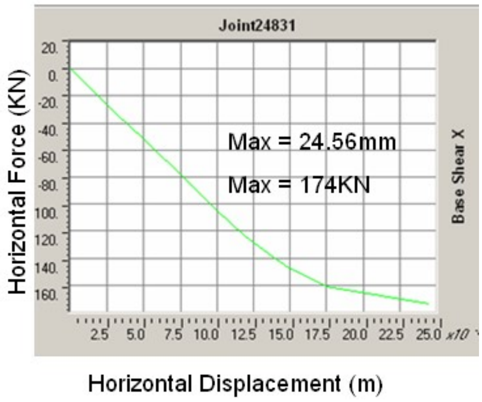

Figure 4a. Horizontal force - Horizontal displacement "bare frame response

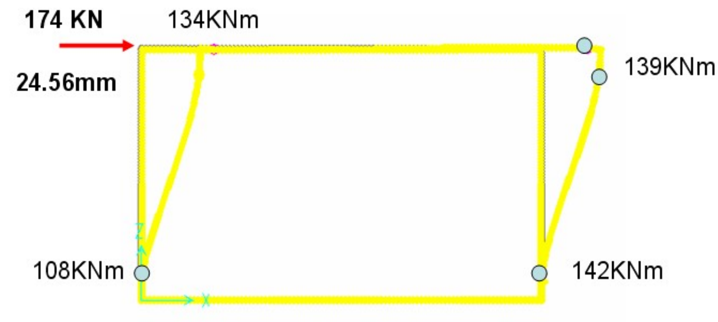

Figure 4b. The studied "bare frame" single-storey one bay R/C frame without the encased R/C panel

Figures 5a and 5b depict the numerically predicted behaviour for the "encased model b". The non-linear trend in the curve representing the variation of the a applied horizontal force at the axis of the top beam against the corresponding displacement, as depicted in figure 5a, is quite evident when the horizontal displacement level exceeds the value of 10mm.

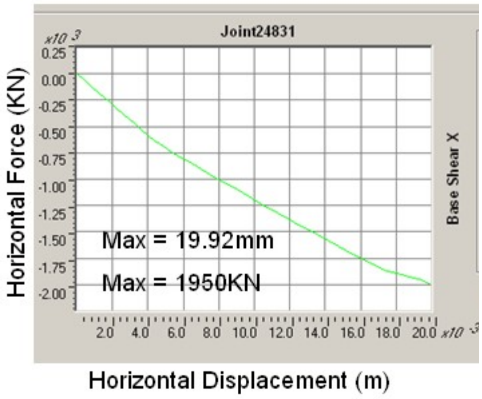

Figure 5a. Horizontal force-displacement "encased model b" response

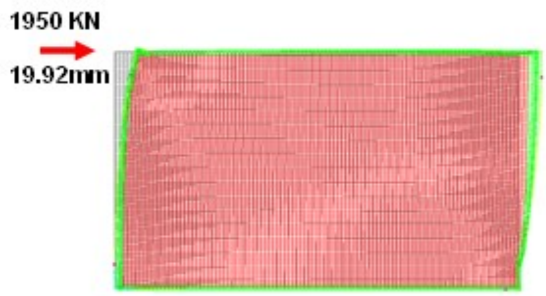

Figure 5b. "encased model b" A single-storey one bay R/C frame with the encased R/C panel connected with contact/gap non-linear links

These non-linear trends are less pronounced here than for the bare frame model. When the top beam horizontal displacement level reaches the maximum amplitude of 19.92mm, the corresponding maximum amplitude of the horizontal force at that level is 1950KN (figure 5b). If this force level is compared to the bearing capacity of the bare frame it, represents an eight (8) times increase. A fifteen (15) times increase, compared to the "bare frame model", can also be observed studying the variation in the stiffness. For the "encased model b" its stiffness reaches the level of 150KN/mm. Figures 6a, 6b, 7a and 7b represent the transfer of forces at the interface between the encased panel and the surrounding frame through the contact/gap mechanism alone [6, 7]. As shown, this transfer takes place at the corners of the encased panel where it contacts the left/right columns (figures 7a and 7b) and the beam/foundation (figures 6a and 6b) near the region of column-to-beam joints whereas a large part of the interface is free of forces due to the gap that forms at the interface at these locations. It can also be seen that these contact forces in a direction normal to the interface reach relatively large amplitude in these narrow column-to-beam joints regions. Such high amplitude forces are expected to introduce additional non-linear mechanisms such as crushing of the encased panel and/or parts of the columns or beams at these regions. These additional mechanisms are not included in this preliminary numerical simulation.

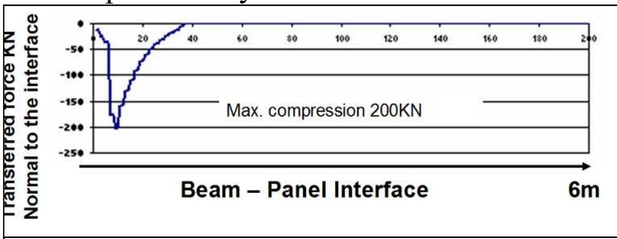

Figure 6a. Transfer of forces normal to the interface between the encased panel and the top beam from the simulation of the encased model b.

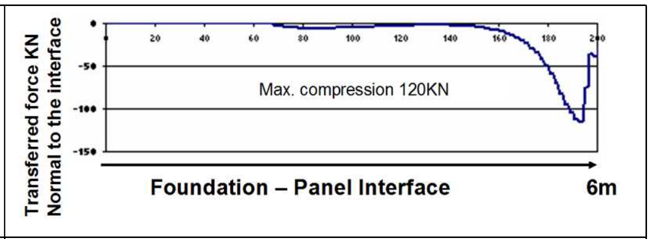

Figure 6b. Transfer of forces normal to the interface between the encased panel and the foundation from the simulation of the encased model b.

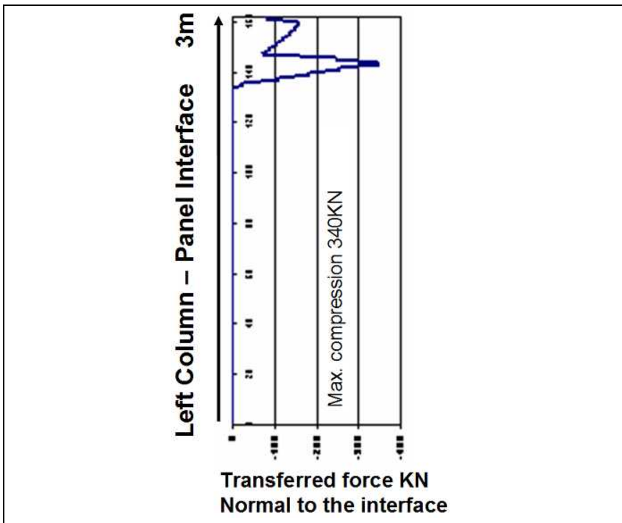

Figure 7a. Transfer of forces normal to the interface between the encased panel and the left column from the simulation of the encased model b.

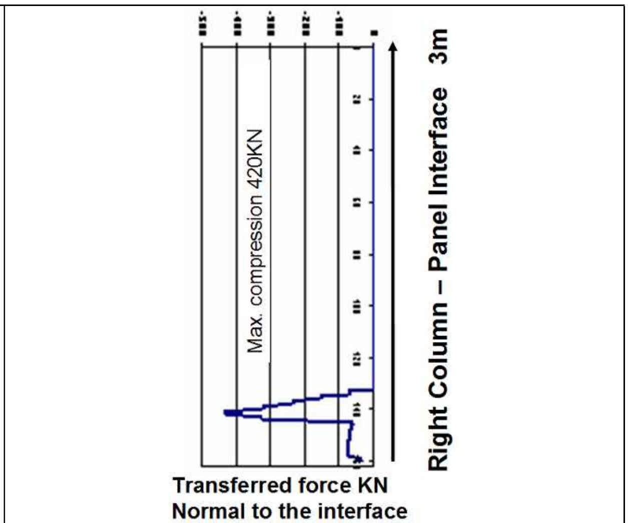

Figure 7b. Transfer of forces normal to the interface between the encased panel and the right column from the simulation of the encased model b.

Figures 8a and 8b depict the numerically predicted behaviour for the “encased model c”. The non-linear trend in the curve representing the variation of the a applied horizontal force at the axis of the top beam against the corresponding displacement, as depicted in figure 8a, is quite evident when the horizontal displacement level exceeds the value of 7.5mm. When the top beam horizontal displacement level reaches the maximum amplitude of 24.95mm the corresponding maximum amplitude of the horizontal force at that level is 4880KN. Apart from the contact/gap mechanism, the presence of steel ties between the encased panel and the surrounding frame both at the top and bottom beam as well as the left and right columns further augments the increase in the bearing capacity and the stiffness. The stiffness reaches the value of 300KN/mm, that represents a thirty (30) times increase compared with the stiffness of the “bare mode”. Figures 6a and 6b represent the transfer of forces at the interface between the encased panel and the surrounding frame through the top beam steel ties whereas figures 9 depict the transfer of forces through the ties that are located at the left and right columns. As can be seen, the transfer takes place partly through the steel ties that are located at the interface between the encased panel and the surrounding frame in a direction parallel to the interface between the encased panel and the surrounding frame left and right columns (figures 10c and 10d) and the beam/foundation (figures 9b). Due to the non-linear properties assumed for the links representing the steel times the maximum force that can be transferred through each one of this link has an upper limit equal to 60KN.

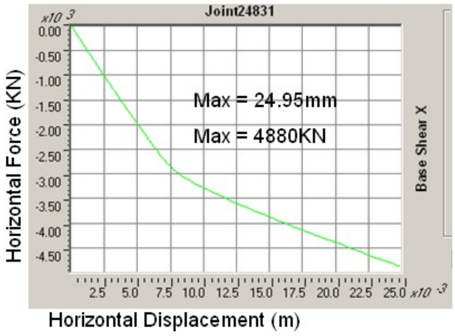

Figure 8a. Horizontal force - displacement "encased model c"

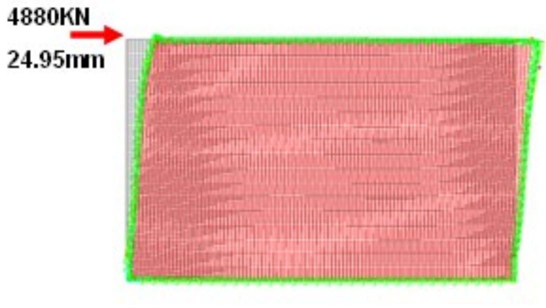

Figure 8b. The "encased model c" single-storey one bay R/C frame with the encased R/C panel

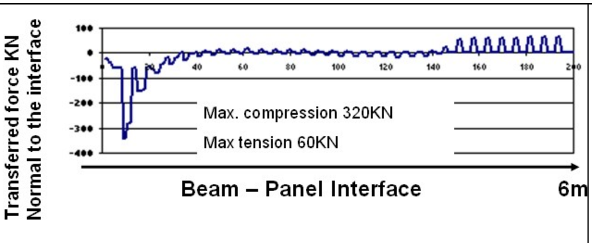

Figure 9a. Transfer of forces normal to the interface between the encased panel and the top beam from the simulation of the encased model c

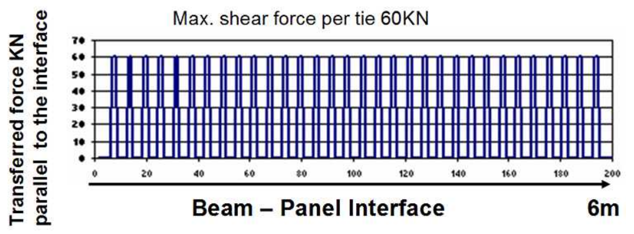

Figure 9b. Transfer of forces parallel to the interface between the encased panel and the top beam from the simulation of the encased model c

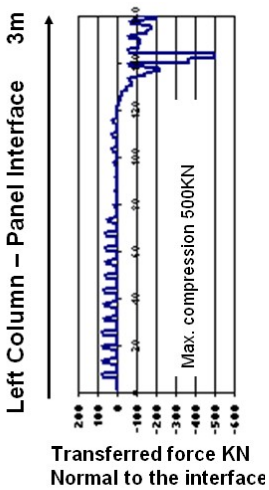

Figure 10a. Transfer of forces normal to the interface between the encased panel and the left column from the simulation of the encased model c

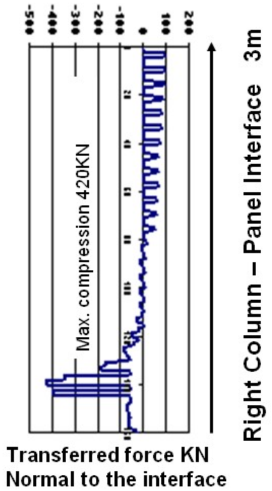

Figure 10b. Transfer of forces normal to the interface between the encased panel and the right column from the simulation of the encased model c

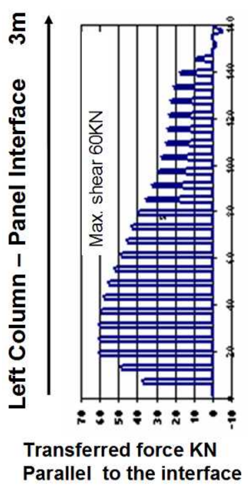

Figure 10c. Transfer of forces parallel to the interface between the encased panel and the left column from the simulation of the encased model c

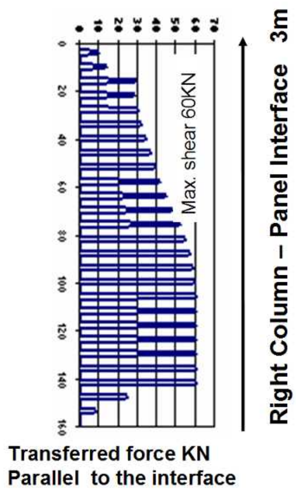

Figure 10d. Transfer of forces parallel to the interface between the encased panel and the right column from the simulation of the encased model c

The contact/gap mechanism when companied with the steel ties mechanism helps also to transfer forces in a direction normal to the interface between the encased panel and the surrounding frame. In figure 9a the forces transferred between the encased panel and the top beam in a direction normal to the interface are depicted. As can be seen the ties help to transfer a limited amount of tensile forces at the right side of the beam; this was not possible when the steel ties were not present (see figure 6a). The compression forces transferred in this case are concentrated again at the left corner of the beam. This time the compressive zone is again narrow with high amplitude (see figures 9a and 6a). The same can also be observed when examining the transfer of forces between the encased panel and the left and right columns in a direction normal to the interface as can be seen by examining figures 7a and 7b (model only with contact/gap mechanism) and figures 10 and 10b (model with contact/gap and metal ties mechanisms). The relative increase in the maximum amplitude values for the compressive forces between "numerical model b" (only contact/gap mechanism) and "numerical model c" contact/gap and metal ties mechanisms) should be seen taking into account that in the later case the horizontal force amplitude is 2.5 times larger than the corresponding amplitude for the former case.

From the preceded preliminary numerical analysis, the encasement of the R/C panel within the single-storey one bay R/C frame resulted in a significant increase of the stiffness and the bearing capacity of the studied system. Moreover, the placement of steel ties apart from increasing the stiffness and the bearing capacity also resulted in moderating the amplitude of the forces that are transferred at the narrow column-to-beam joints regions in a direction normal to the interface through the contact/gap mechanism. Such moderation in the amplitude of the transferred forces at the interface will mitigate the possibility of crushing of the encased panel and/or parts of the columns or beams at these regions. It can also be concluded that the presence of steel ties in the interface between the encased R/C panel and the surrounding R/C frame has an overall beneficial effect on the behaviour of this type of structural system to seismic type loading. As shown in the preliminary numerical study when there are steel ties in such an interface these ties will transfer forces in a direction normal and parallel to the interface simultaneously. The level of these forces may vary in amplitude as well as in direction during the loading of the structure in a cyclic seismic type of loading. An experimental investigation was carried out with its main objective to study the mechanism of the transfer of such forces at the interface in such a way that this mechanism can be described both in terms of bearing capacity at a limit-state level linked with failure modes that are expected to appear. A summary of this study is presented in the next section. It must be underlined that in the preliminary numerical analysis, apart from the non-linear mechanisms that were used to numerically simulate the transfer of forces at the interface between the encased panel and the surrounding frame as well as the simulation of the flexural plastic hinges at predetermined locations at the ends of the columns and beams the possibility of non-linear behaviour of the encased panel itself, although very significant, was ignored at present.

3 EXPERIMENTAL SEQUENCE

Summary results will be presented in this session from an extensive experimental sequence which aimed to study the interaction between metal ties at the interface between the encased R/C panel and the surrounding frame [7]. As described in the introduction, as a first step the structural members of the R/C frame would be jacketed (figure 2a) and then the encased panel will be constructed within the bay of this strengthened R/C frame either with or without metal ties (see section 2). Figure 10a depicts the sketch of such an encased R/C frame with columns and beams having jackets before the placement of the encased R/C panel. In this figure, sections of this encasement is also shown between the R/C panel and either the left/right column or the top/bottom beam. Figure 10b shows also this connection detail for the left column. It can be easily seen that this detail can also represent the connection between the encased panel with the right column (180 deg. rotation) or with the top and bottom beams (90 deg. or 270 deg. rotation, respectively (figures 11a and 11b). The dimensions shown in figure 10b are the ones selected to be used to construct the specimens to be tested at the laboratory. These dimensions represent an R/C member of relatively small dimensions. As already explained, such a specimen represents a portion of an R/C encased panel (200mm thick) connected with a portion of a column/beam of the surrounding frame with or without the use of steel ties. When steel ties are used they are embedded at the mid-plane of the panel and are anchored to the mass of the old concrete of the column (220mm by 220mm), which is also retro-fitted with a jacket 60mm thick. Both the jacket and the R/C encased panel are indicated in a different color in figure 10b in order to differentiate the new concrete from the existing column (old concrete). This specimen was loaded as indicated in figure 11b, 11c and 11d. A load was applied normal to the interface (horizontal in figures 11b, 11c and 11d) whereas at the same time an additional load was applied in a direction parallel to the interface (vertical in figures 11b, 11c and 11d). This connection detail is studied with a specimen having a height of 540mm, with the encasement being 260mm high. This limitation was introduced in order to confine the examination in the connection with a metal tie and control the forces to be transferred.

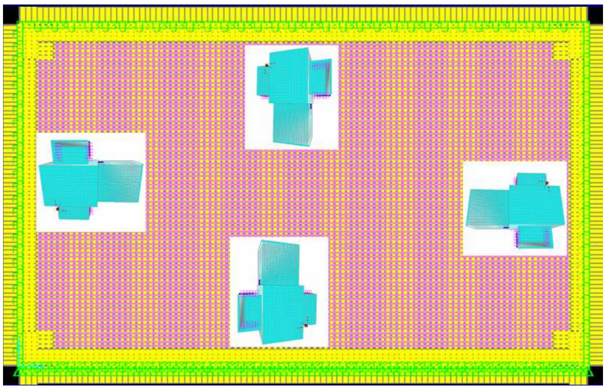

Figure 11a. Sketch of an encased R/C panel and frame having columns and beams with jackets

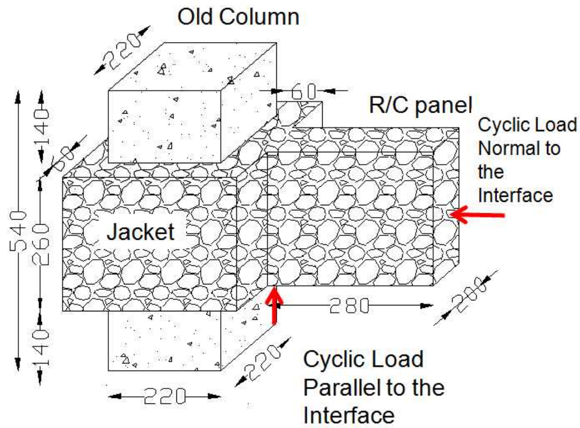

Figure 11b. Specimen of a portion of an encased R/C panel and the jacketed column

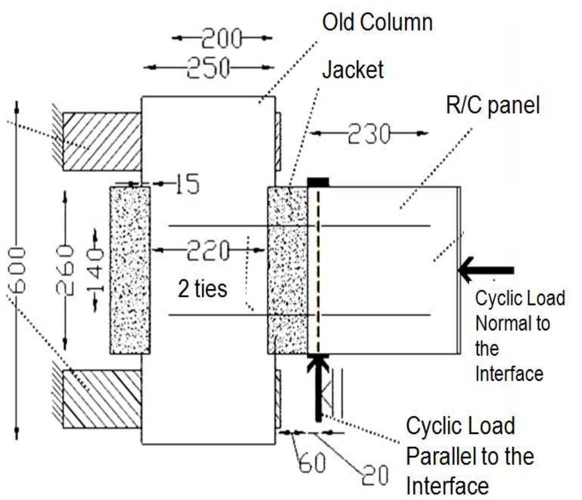

Figure 11c. Loading arrangement of a portion of encased R/C panel and the jacketed column

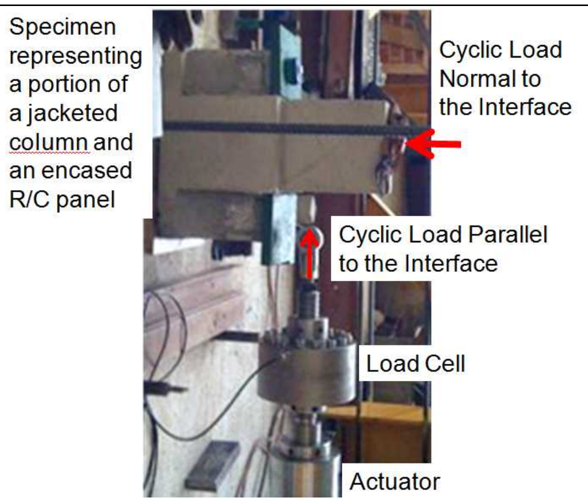

Figure 11d. Loading arrangement of a portion of encased R/C panel and the jacketed column

The load which was applied parallel to the interface was varied in time in a manner consisting of three sinusoidal cycles of constant amplitude with a frequency 0.1Hz. The load that was applied normal to the interface was either kept constant at a predetermined level (tension or compression) or it was also varied in the same way as the load applied parallel to the interface. This type of combined loading was thought to represent the transfer of forces at such an interface with the presence of steel ties, as was found by the preliminary numerical analysis described in a summary form in section 2. The total loading sequence per specimen consisted of a series of such cycles with continuously increasing amplitude till the failure of the specimen. This type of combined cyclic loading is believed to be adequately representative of the stress field that is expected to develop at this part of the encasement from the transfer of forces between the encased R/C panel and the surrounding frame. Such forces will arise from the seismic response of a multi-story R/C structure and it is assumed that will subject an encased R/C frame mainly to this type of in-plane loads, ignoring the forces that would result in the out-of-plane direction of this encased R/C frame.

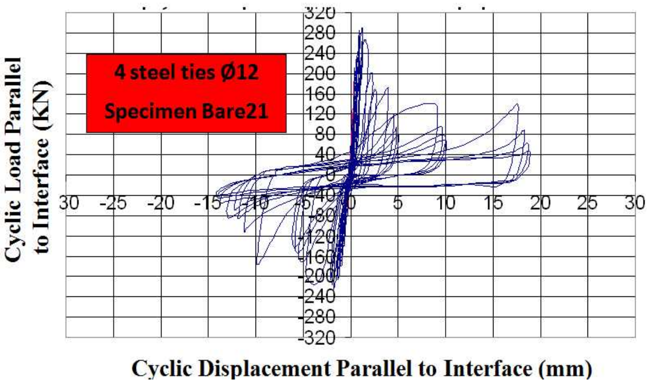

Figure 12a. Measured Load-displacement cyclic response in direction parallel to the interface

Figure 12b. Deformed shape of the steel ties at the final stage of loading sequence.

Figure 12a depicts such measured response for one of the specimens, with 4 steel ties of 12mm diameter. In this figure, the load applied in the direction parallel to the interface is plotted in the ordinates whereas the measured resulting sliding displacement at the interface between the portion of the panel and the jacketed column is plotted at the abscissa of this figure. Instrumentation was provided to measure the variation of the applied loads as well as the deformation of the specimen during such a loading sequence. Due to the stress field arising at the vicinity of this interface when the previously described combined loading is applied, the expected modes of failure include a shearing pattern for the concrete volume neighbouring the steel ties accompanied by a local deformation of the steel ties themselves. The amplitude of the applied force parallel to the interface was gradually increased in cyclic manner. This is consistent with a variation of the horizontal forces resulting from seismic actions.
As can be seen in figure 12a, the measured response reveals three stages in the performance of such a steel-tie connection. Up to a relatively small cyclic displacement level, of the order of 1.0mm, the measured response is almost linear elastic. Then, increasing the displacement/load amplitude the maximum capacity of the connection is reached. The sliding deformations at the interface are relatively small including a portion of remaining plastic deformations. Finally, these plastic deformations increase substantially accompanied by a significant drop in the bearing capacity. Excessive cracking of the interface occurs that reveals the deformed shape of the steel ties, as they are shown in figure 12b after the end of the test and the destruction of the specimen. The measured response of this steel tie connection at the interface, in a direction parallel to the interface, under a combined loading representative of the stress field that is expected to develop at this part of the encasement, is up to a point in agreement with the assumptions made in the preliminary numerical simulation presented in section 2.

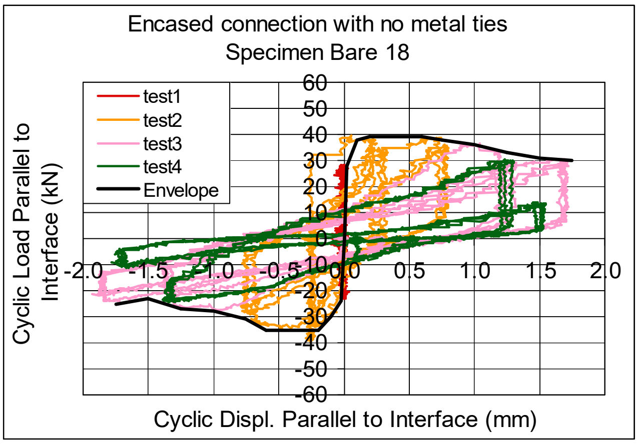

Figure 13a. Measured Load-displacement cyclic response in direction parallel to the interface

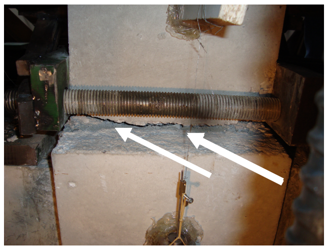

Figure 13b. Broken interface at the end of test for specimen 18 without metal ties

Figure 13c. Broken interface at the end of test for specimen 18 without metal ties

Figure 13a depicts the measured response for one of the specimens without any steel ties. The observed state of the interface at the end of this test is depicted in figures 13b and 13c. Again, the load applied in the direction parallel to the interface is plotted in the ordinates whereas the measured resulting sliding displacement at the interface between the portion of the panel and the jacketed column is plotted at the abscissa in this figure. By comparing the load-displacement response of figure 13a with the corresponding load-displacement response of figure 12a the contribution of the presence of the steel ties can be clearly identified. The obtained bearing capacity with the four 12mm diameter steel ties is approximately seven (7) times larger than where the ties are not there. This maximum capacity without the ties is observed for very small amplitude sliding displacement. This sliding displacement amplitude is less than 20% of the corresponding displacement amplitude that the maximum capacity was observed when the steel ties were in place. Furthermore, the degradation of the bearing capacity when the sliding displacement amplitude is increased is far more pronounced without the steel ties than when the steel ties are present. This simple comparison demonstrates the importance of the presence of the steel ties in transferring the combined forces at the interface between the encased R/C panel and the jacketed columns or beams of the surrounding R/C frame. A next important step is to be able to quantify such a transfer of forces for connection details that can be used in design. This is done in the following section whereby a numerical simulation of the tested connection detail is examined in an effort to validate simple numerical tools that can serve such a purpose.

4 NUMERICAL SIMULATION OF THE STUDIED CONNECTION DETAIL

In what follows a simple numerical simulation of the tested connection detail is examined [7]. The geometry of this detail is the one shown in figures 11b and 11c.

4.1. Non-linear interaction of the steel ties with the interface of the encased panel and the column

As can be seen in figure 13b the interface is introduced as a line separating completely the R/C encased panel from the jacketed column that are simulated by 2-D linear elastic finite elements.

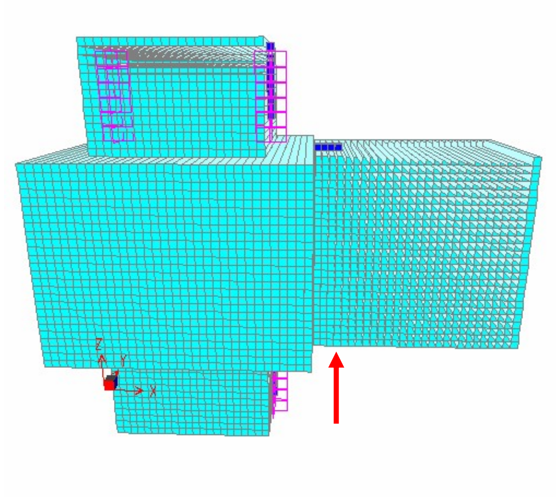

Figure 14a. 3-D Finite element representation of the tested connection.

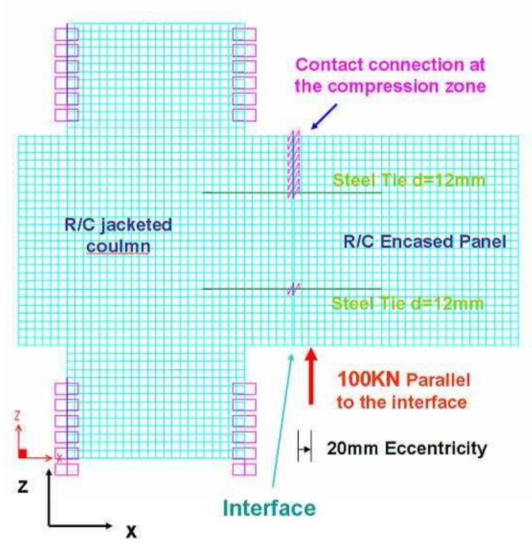

Figure 14b. 2-D Finite element representation of the tested connection. The placement of the steel ties is indicated

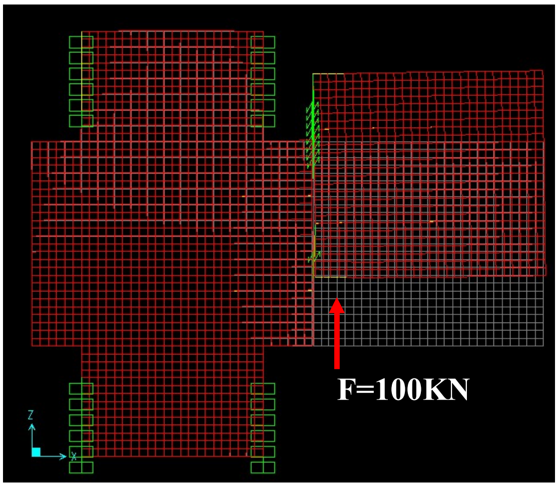

A). Magnified displaced shape.

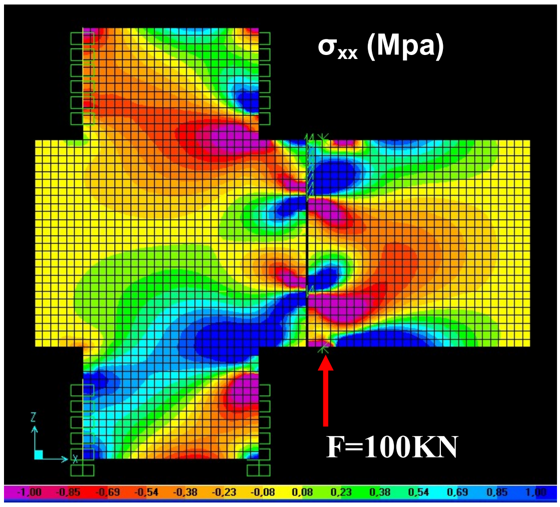

b). σ_{xx} stress distribution (F=100KN)

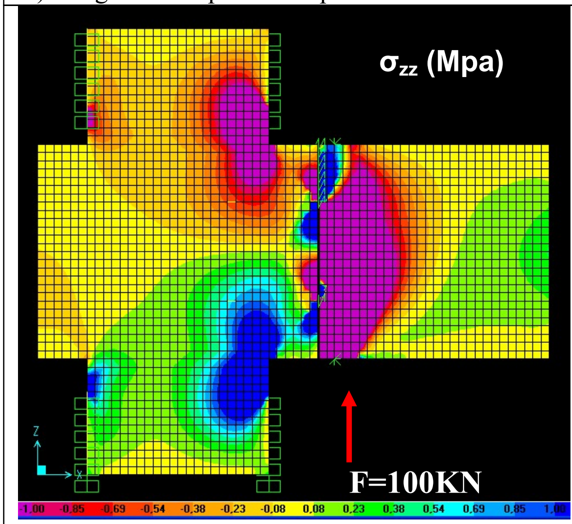

c). σ_{zz} stress distribution (F=100KN)

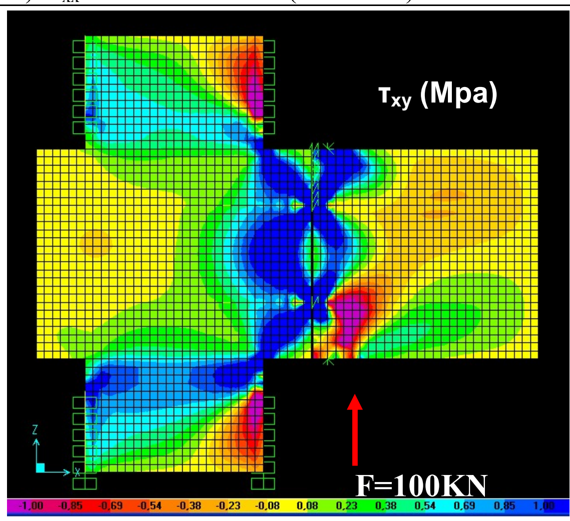

d). τ_{xz} stress distribution (F=100KN)

Figure 15. Displacement and stress distribution of the interaction between the R/C encased panel and the R/C jacketed column when subjected to 100KN force parallel to the interface. R/C encased panel free to displace x-x

The load parallel to the interface is applied with a 20mm eccentricity in the same way that was applied during testing. A number of contact/gap elements were used to connect the R/C encased panel with the R/C jacketed column at the upper part of the interface, as shown in figure 14b. The R/C jacketed column was supported in its upper and lower part with fixed boundary conditions thus replicating the actual support conditions of the tested specimens (see figures 11c and 11d). Two distinct cases were examined with reference to the R/C encased panel possibility to displace in the x-x direction. In the first case the R/C encased panel was left free to displace in this direction whereas in the second case this displacement freedom of the R/C encased panel was restrained. The applied load was introduced in a step-by-step manner. The resulting displacement and stress distribution is depicted in figures 15a to 15d for the case when the R/C encased panel can displace in the x-x direction whereas figures 16a to 16d depict the displacement and stress distribution when the encased panel is restrained in the x-x direction. Both these figures depict the displacement and stress state of stress when the force parallel to the interface reaches the amplitude of 100KN

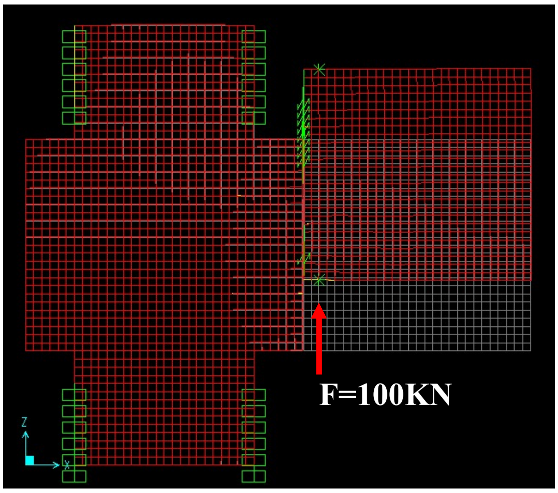

a). Magnified displaced shape.

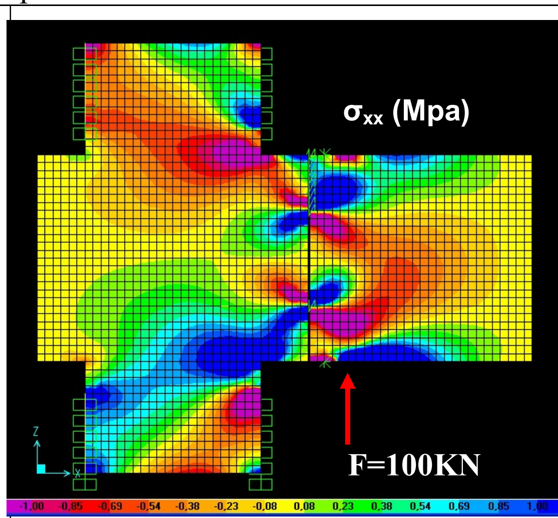

b). σ_{xx} stress distribution (F=100KN)

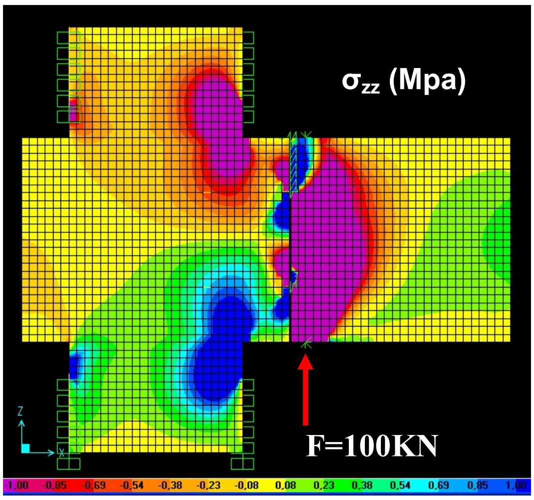

c). σ_{zz} stress distribution (F=100KN)

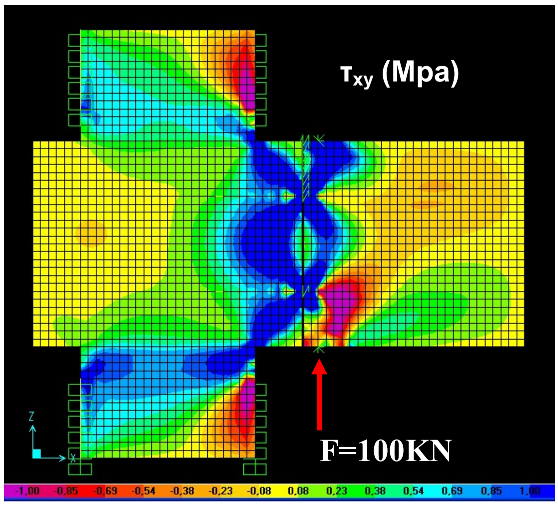

d). τ_{xz} stress distribution (F=100KN)

Figure 16. Displacement and stress distribution of the interaction between the R/C encased panel and the R/C jacketed column when subjected to 100KN force parallel to the interface. R/C encased panel restrained to displace x-x

The connection of these two parts is accomplished by non-linear links representing two steel ties having a diameter of 12mm and a yield stress of 500MPa. They are located as shown in figure 14b. These two non-linear links at the interface are connected to linear frame elements representing the same steel ties extending to either side of the interface within the R/C encased panel and the R/C jacketed column, as also indicated in the same figure.
As can be seen in both these figures the presence of the steel ties results in a considerable stress concentration of these parts of the concrete volume that are neighbouring the steel ties. Therefore, in order to predict realistically the bearing capacity of such a connection it is necessary to numerically simulate not only non-linear interaction of the steel ties with the interface but also the non-linear interaction of these steel ties with the concrete volume that they are embedded to. This is briefly described in the next session.

4.2. Non-linear interaction of the steel ties with the interface as well as with the volume of concrete of the encased panel and the column

In this numerical simulation effort a more complex model was developed [7]. This was a 3-D representation of the problem at hand. The interface was simulated with a contact area and the metal ties with 3-D rods that were embedded in the 3-D finite element mesh in an exact geometric representation of the actual specimen with four (4) steel ties having a diameter of 12mm each. Due to symmetry with respect to the y-z plane only one half (1/2) of the specimen was numerically simulated. This is shown in figure 17.

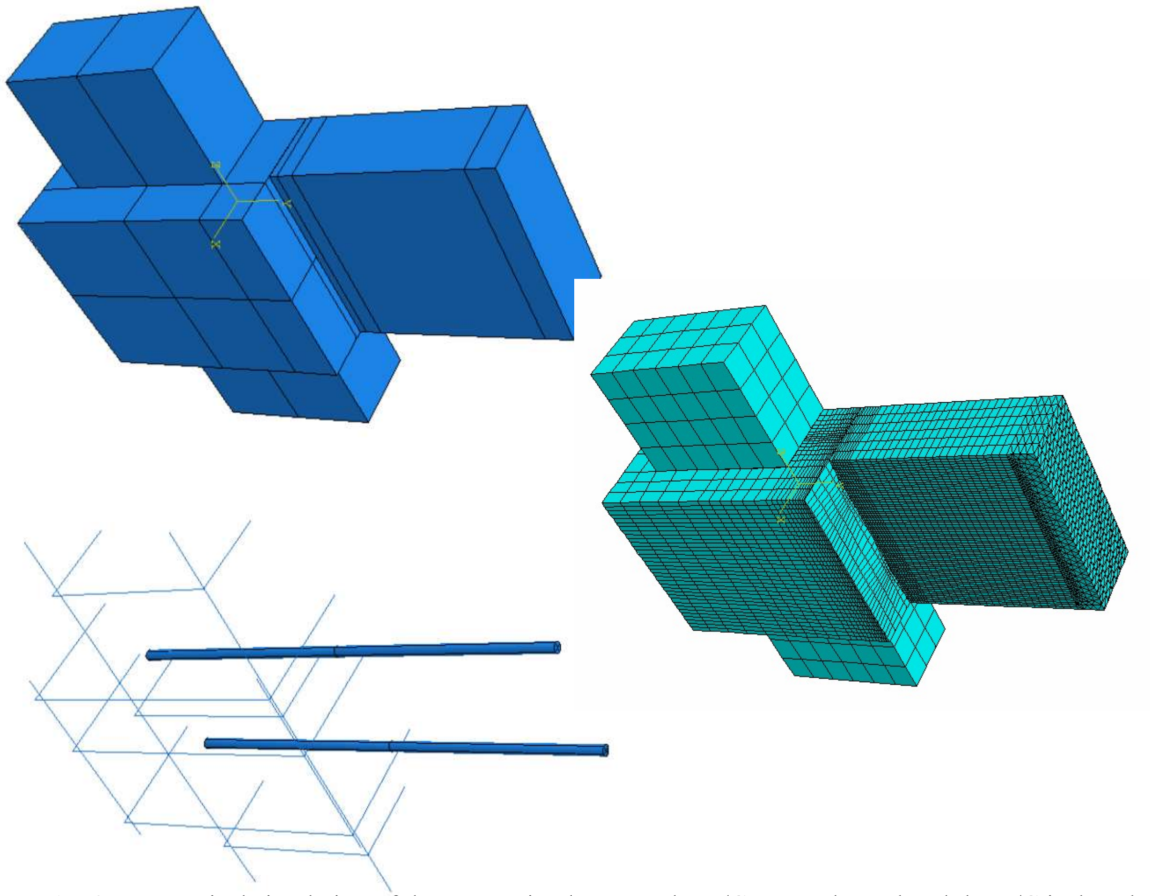

Figure 17. 3-D numerical simulation of the connection between the R/C encased panel and the R/C jacketed column with four (4) steel ties having a diameter of 12mm each.

The material low adopted for the steel ties was elasto-plastic with isotropic post-yield including true stress - logarithmic plastic strain. This material law was based on the measured behaviour if steel specimens identical to the used steel ties which were tested under axial tension. Similar procedure was followed for the reinforcing bars included in the R/C encased panel and jacketed column despite the fact that these bars were not stressed beyond the elastic range. For the concrete damaged plasticity model was adopted (Abaqus [9]). An analytical description of this material model is given by Malm (2009) [11] and Mercan et al. 2010 [12]. The Young's modulus and the compressive concrete stress-strain behaviour were again based on measurements obtained from uni-axial compression of concrete cylinders that were constructed with the same mix and at the same time with the tested specimens of section 2. Based on these measurements the Poisson's ratio is equal to 0.15 and the tensile strength (f_{ctm}), according to EN 1992-1-1 [10], is equal to 2.2 MPa.

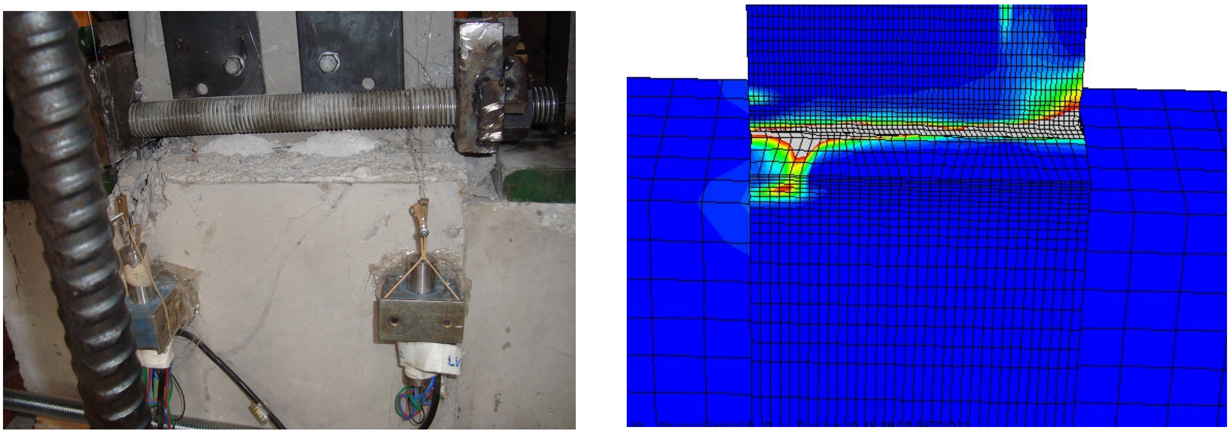

Figure 18. The formation of the cracked concrete region neigbouring the interface (observed and predicted).

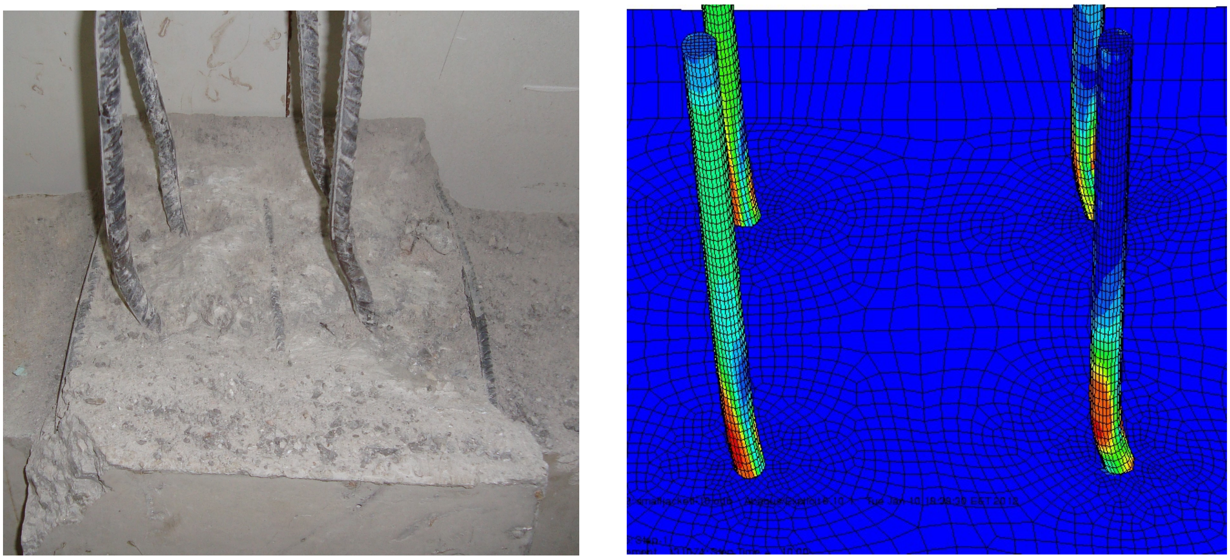

Figure 19. The observed and the numerically predicted deformation and stress patterns of the steel ties in the region neighbouring the interface.

At the right part of figure 18 the cracked concrete region reigbouring the interface is depicted when the applied force results in a sliding displacement equal to 4mm. At the left side of the same figure the observed cracked concrete region near the interface is also shown for similar amplitude of the sliding displacement (see figure 12a). As can be seen in figure 18 the nu-

merical prediction is a realistic simulation of the observed behaviour of the concrete volume in the region neighbouring the interface.
At the right part of figure 19 the numerically predicted deformation and stress patterns of the steel ties in the region neighbouring the interface is depicted when the sliding displacement reached the maximum amplitude (larger than 10mm). At the left part of the same figure the observed deformed steel ties at the end of the test are also shown (see also figure 12b). As can be seen in figure 19, the predicted steel tie deformation/stress pattern is a realistic simulation of the observed behaviour of the steel ties in the region neighbouring the interface. This is also shown by figures 20a and 20b.

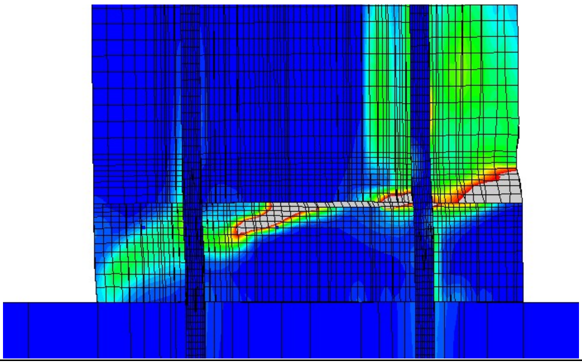

Figure 20a. Propagation of the cracked (plastified) concrete at the region neigbouring the interface together with the deformed shape of the steel ties

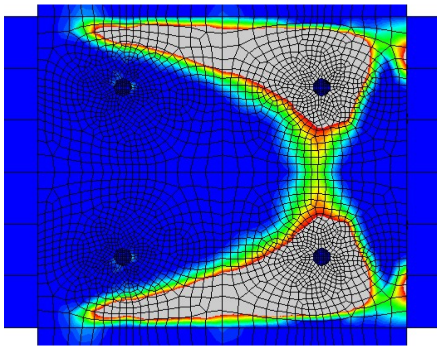

Figure 20b. Spreading of the cracked (plastified) concrete at the region neighboring the interface

In figure 21 the measured envelope curve of the variation of the applied force parallel to the interface versus the resulting sliding displacement is plotted together with the corresponding numerically predicted force-displacement response. As can be seen in this figure the measured load-displacement response of the examined connection is reasonably well predicted by the described numerical simulation.

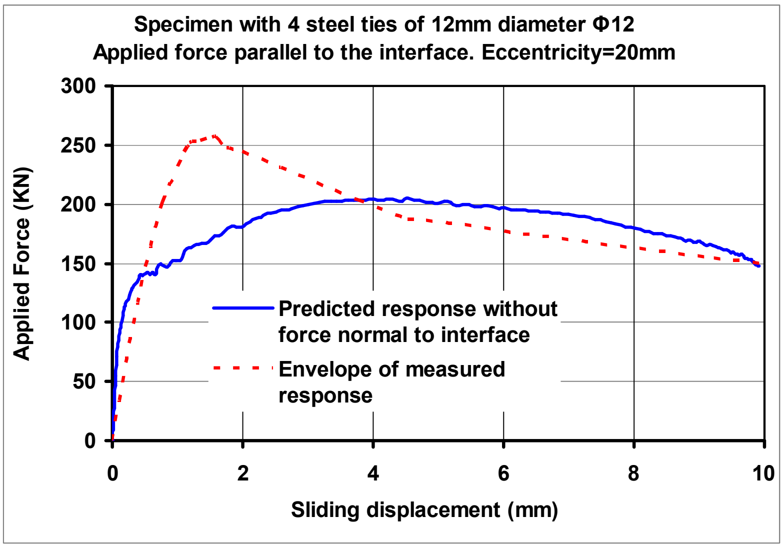

Figure 21. Measured and predicted applied force parallel to the interface versus sliding displacement response

The maximum predicted bearing capacity value is approximately 20% smaller than the corresponding measured value. Moreover, the measured response appears to have a stiffer behaviour till it reaches its maximum resistance than the predicted response. Despite this discrepancy, the predicted behaviour for both the initial stiff part (for sliding displacement amplitudes smaller than 0.5mm) as well as for the plastic part (for sliding displacement amplitudes larger than 3mm) agree quite well with the measures response of the tested specimen. Based on the above discussion between predicted and observed response it can be concluded that the described in this section numerical simulation is a quite valid numerical approach that can be further utilized towards quantifying the transfer of forces for connections details that are studied in the present work in order to be used in design.

5 CONCLUSIONS

• This numerical study examines the influence on the in-plane behaviour of one-bay single-storey reinforced concrete (R/C) frame arising from the presence of an encased R/C panel with or without steel ties.
• From the preliminary numerical analysis results it can be concluded that such an encasement results in a considerable increase of the stiffness and the bearing capacity of the studied system, especially when steel ties are present at the interface. Moreover, the placement of steel ties also moderates the amplitude of the forces that are transferred at the narrow column-to-beam joints regions in a direction normal to the interface through the contact/gap mechanism, and consequently, mitigate the possibility of crushing of the encased panel and/or parts of the columns or beams at these regions.
• Thus, it can be concluded that an encased R/C panel, connected with the appropriate steel ties to the surrounding R/C frame, has an overall beneficial effect on the behaviour of this type of structural system to seismic type loading
• An experimental sequence was also performed in order to quantify the behaviour of such steel tie connections at the interface under a stress field that is expected to develop at this part of the encasement during seismic type loading. Such measured behaviour, is in agreement with the assumptions made concerning the behavioural characteristics of these steel ties in the preliminary numerical analysis.
• A more advanced numerical simulation was also examined that includes the plastification of the steel ties as well as that of the concrete volume utilizing the capabilities of the damaged plasticity model of the commercial software Abaqus. It was demonstrated that the predicted plastic strain and deformation patterns for the steel ties and the concrete in the regions neighbouring the interface were a realistic representation of the corresponding observed behaviour. Moreover, the predicted applied force parallel to the interface versus the sliding displacement response agrees reasonably well with the measured response in terms of stiffness, maximum bearing capacity and plastified sliding deformations.
• Based on the above discussion between predicted and observed response it can be concluded that the described advanced numerical simulation is a quite valid numerical approach that can be further utilized towards quantifying the transfer of forces for connections details that are studied in the present work in order to be used in design.

ACKNOWLEDGEMENTS

The partial support of the Hellenic Organization of Earthquake Planning and Protection is gratefully acknowledged.

- To the memory of Ray W. Clough, Professor Emeritus of the University of California, at Berkeley, U.S.A.

REFERENCES

[1] Manos. G.C., Soulis V. J., J. Thauampteh. "A Nonlinear Numerical Model and its Utilization in Simulating the In-Plane Behaviour of Multi-Storey R/C frames with Masonry Infills", *The Open Construction and Building Technology Journal,6,* (Suppl 1-M16) 254-277,2012.

[2] Manos. G.C., Soulis V.J., Thauampteh J., "The Behaviour of Masonry Assemblages and Masonry-infilled R/C Frames Subjected to Combined Vertical and Cyclic Horizontal Seismic-type Loading", Journal of Advances in Engineering Software, Vol. 45, pp. 213-231, 2011. 12.

[3] Manos George, "Consequences on the urban environment in Greece related to the re-cent intense earthquake activity", Int. Journal of Civil Engineering and Architecture, Dec. 2011, Volume 5, No. 12 (Serial No. 49), pp. 1065–1090.

[4] Organization of Earthquake Planning and Protection of Greece (OASP), Guidelines for Level—An earthquake performance checking of buildings of public occupancy, published by OASP, Athens, 2001.

[5] Provisions of Greek Seismic Code (2000), Organization of Earthquake Planning and Protection of Greece (OASP), Dec. 1999, published by OASP. Revisions of seismic zonation introduced in 2003, Government Gazette, Δ17α /115/9/ΦN275, No. 1154, Athens, 12 Aug. 2003.

[6] Manos G.C., Soulis V., Katakalos K., Koidis G. (2013), "Numerical and Experimental study of seismic retrofitting for one-bay single-storey reinforced concrete (R/C) frames with an encased R/C panel", Computational Methods and Experimental Measurements XVI Journal, Vol. 55, pp. 39-411.

[7] G.C. Manos (2012) "Cyclic In-plane Behaviour of R/C Frames Retrofitted with Jacketing and an Encased R/C Panel" Report to Hellenic Earthquake Planning and Protection Organization (EPPO) in Greek

[8] Organization of Earthquake Planning and Protection of Greece (OASP), Guidelines for Retrofitting in Reinforced Concrete Buildings, Government Gazzette, Δ17α /04/5/ΦN 429-1, No 42, Athens, 20 Jan. 2012.

[9] Hibbitt, Karlsson, Sorensen. Inc. ABAQUS user's manual volumes I–V and ABAQUS CAE manual. Version 6.10.1. Pawtucket, USA; 2010.

[10] EN 1992-1-1 (2004). Eurocode 2:Design of Concrete structures-Part 1.1: General rules and rules for buildings. CEN.

[11] Malm R. (2009). Predicting shear type crack initiation and growth in concrete with non-linear finite element method. PhD thesis, Department of Civil and Architectural Engineering, Royal Institute of Technology (KTH) Stockholm.

[12] Mercan B., Schultz A.E. and Stolarski H.K. (2010). Finite element modeling of pre-stressed concrete spandrel beams. Engineering Structures 32 (9), 2804-2813.